RESPONSE ANALYSIS OF AN ELASTIC FLEXIBLE BASE MAT RESTING ON THE SURFACE OF MULTI-LAYERED STRATA

F.SASAKI (1)
T.OHTA (2)
K.MASUDA (1)
K.MIURA (2)
Presenting Author: F.SASAKI

SUMMARY

This paper describes the numerical procedures to analyze the dynamic soil-structure interaction of the elastic base mat resting on the surface of multi-layered strata. There were no previous methods proposed to analyze the dynamic soil-structure interaction under above-mentioned conditions. The effects of elastic deformations of base mat and the existence of strata on the dynamic soil-structure interaction are shown through solving a representative example.

INTRODUCTION

This paper describes the numerical procedures to analyze the dynamic soil-structure interaction (DSSI) of the elastic base mat resting on the surface of multi-layered strata. The effects of strata and elastic deformations of base mat on DSSI will be discussed. DSSI have direct effects on the dynamic characteristics of rigid structures such as the nuclear reactor buildings (R/B). The precise estimates of these effects inevitably require to investigate the aseismic safety of R/B. Many methods (Ref.1,2,3,4,5,6) have been proposed to estimate the effects of DSSI. But most of these contain the following analytical assumptions. Soil is a semi-infinite isotropic homogeneous medium, and the base mat of R/B is perfectly rigid or the contact pressures between the base mat and soil are assumed a priori. The numerical results performed under above-mentioned assumptions are considerably different from experimental results of R/B. The real soil underlying R/B consists of multi-layered strata that have different physical constants. The existence of strata and elastic deformations of base mat may have an important role for DSSI.

MATHEMATICAL FORMULATION

The integral equations must be solved to analyze the soil-structure interaction problems. These equations have kernels which express the relations between point loads applying on the surface of soil and displacements due to these loads. The kernels are usually named by Green's functions. Green's functions for a vertical load can be introduced as follows. In the case of a horizontal load, these are formulated in a similar manner. The soil is assumed to be horizontally multi-layered strata. Each stratum is an isotropic homogeneous medium with hysteresis type dampings. The geometric configuration of soil and coordinate systems

(1) Information Processing Center, Kajima Corporation, Tokyo, Japan

(2) Kajima Institute of Construction Technology, Tokyo, Japan

are shown in Fig.1. The general solutions of wave propagation equations for m-th layer are expressed by Eq.(1).

$$[u_r^m(\tilde{r},\tilde{z}_m), u_z^m(\tilde{r},\tilde{z}_m), \sigma_z^m(\tilde{r},\tilde{z}_m), \tau_{rz}^m(\tilde{r},\tilde{z}_m)]^T = \int_0^\infty [\tilde{u}_r^m(\tilde{z}_m)J_1(\xi\tilde{r}), \tilde{u}_z^m(\tilde{z}_m)J_0(\xi\tilde{r}), \mu_1 j_1 \tilde{\sigma}_z^m(\tilde{z}_m)J_0(\xi\tilde{r}), \mu_1 j_1 \tilde{\tau}_{rz}^m(\tilde{z}_m)J_1(\xi\tilde{r})]^T d\xi \quad (1)$$

in which, $J_k(\ )$ = The first kind of Bessel function of k-th order
$\tilde{r}=\omega r/C_{T1}$, $\tilde{z}_m=\omega z_m/C_{T1}$, $j_1=\omega/C_{T1}$, ω = circular frequency
C_{T1} = S-wave velocity of first stratum
μ_1 = shear rigidity of first stratum

Matrix elements of right hand of Eq.(1) are given by (2).

$$\boldsymbol{W}_m = \boldsymbol{Q}_m \boldsymbol{B}_m \quad (2)$$

where $\boldsymbol{W}_m = \{\tilde{u}_r^m(\tilde{z}_m), \tilde{u}_z^m(\tilde{z}_m), \tilde{\sigma}_z^m(\tilde{z}_m), \tilde{\tau}_{zr}^m(\tilde{z}_m)\}^T$
$\boldsymbol{B}_m = \{A_m, j_1 C_m, B_m, j_1 D_m\}$

$$\boldsymbol{Q}_m = \frac{1}{\tilde{C}_m^2} \begin{vmatrix} \frac{\xi E_1}{n_m^2 g_{pm}} & -\frac{\xi\tilde{\beta}_m E_2}{g_{sm}} & \frac{\xi E_3}{n_m^2 g_{pm}} & \frac{\xi\tilde{\beta}_m E_4}{g_{sm}} \\ \frac{\tilde{\alpha}_m E_1}{n_m^2 g_{pm}} & -\frac{\xi^2 E_2}{g_{sm}} & -\frac{\tilde{\alpha}_m E_3}{n_m^2 g_{pm}} & -\frac{\xi^2 E_4}{g_{sm}} \\ \frac{(\tilde{C}_m^2 g_{sm}-2\xi^2)E_1}{\tilde{\mu}_m g_{sm} n_m^2 g_{pm}} & \frac{2\tilde{\beta}_m\xi^2 E_2}{\tilde{\mu}_m g_{sm} g_{sm}} & \frac{(\tilde{C}_m^2 g_{sm}-2\xi^2)E_3}{\tilde{\mu}_m g_{sm} n_m^2 g_{pm}} & -\frac{2\tilde{\beta}_m\xi^2 E_4}{\tilde{\mu}_m g_{sm} g_{sm}} \\ \frac{-2\tilde{\alpha}_m\xi E_1}{\tilde{\mu}_m g_{sm} n_m^2 g_{pm}} & \frac{\xi(2\xi^2-\tilde{C}_m^2 g_{sm})E_2}{\tilde{\mu}_m g_{sm} g_{sm}} & \frac{2\tilde{\alpha}_m\xi E_3}{\tilde{\mu}_m g_{sm} n_m^2 g_{pm}} & \frac{\xi(2\xi^2-\tilde{C}_m^2 g_{sm})E_4}{\tilde{\mu}_m g_{sm} g_{sm}} \end{vmatrix}$$

A_m, B_m, C_m, D_m = undetermined coefficients
$E_1=\exp(-\tilde{\alpha}_m\tilde{z}_m)$, $E_2=\exp(-\tilde{\beta}_m\tilde{z}_m)$, $E_3=\exp(\tilde{\alpha}_m\tilde{z}_m)$, $E_4=\exp(\tilde{\beta}_m\tilde{z}_m)$
$\tilde{\alpha}_m=\sqrt{\xi^2-\tilde{C}_m^2 n_m^2 g_{pm}}$, $\tilde{\beta}_m=\sqrt{\xi^2-\tilde{C}_m^2 g_{sm}}$, $\tilde{C}_m=C_{T1}/C_{Tm}$, $n_m=C_{Tm}/C_{Lm}$
$\tilde{\mu}_m=\mu_1/\mu_m$, $g_{sm}=[1+i\mu'_m/\mu_m]$, $g_{pm}=[1+i(\lambda_m'+2\mu_m')/(\lambda_m+2\mu_m)]^{-1}$
C_{Lm} = P-wave velocity of m-th stratum
$\mu_m+i\mu'_m$ = complex rigidity of m-th stratum
$(\lambda_m+2\mu_m)+i(\lambda_m'+2\mu_m')$ = complex rigidity of P-wave of m-th stratum

And now, for the value $\boldsymbol{W}_m$, $\boldsymbol{Q}_m$ of top of m-th stratum and bottom of m-th stratum, following notations are introduced.

$$\boldsymbol{W}_{m,m-1}=\boldsymbol{W}_m|_{\tilde{z}_m=0}, \quad \boldsymbol{W}_{m,m}=\boldsymbol{W}_m|_{\tilde{z}_m=d_m} \quad (3)$$

$$\boldsymbol{C}_m=\boldsymbol{Q}_m|_{\tilde{z}_m=0}, \quad \boldsymbol{D}_m=\boldsymbol{Q}_m|_{\tilde{z}_m=d_m} \quad (4)$$

where $d_m=\omega H_m/C_{T1}$

Then next relation is obtained.

$$\boldsymbol{B}_{N+1}=\boldsymbol{J}_N\boldsymbol{W}_{1,0} \quad (5)$$

where $\boldsymbol{J}_N=\boldsymbol{C}_{N+1}^{-1}\cdot\boldsymbol{D}_N\cdot\boldsymbol{C}_N^{-1}\cdot\boldsymbol{D}_{N-1}\cdot\boldsymbol{C}_{N-1}^{-1}\cdots\boldsymbol{D}_1\cdot\boldsymbol{C}_1^{-1}$

And dividing Eq.(5) into two part, Eq.(5) reduces to Eq.(6).

$$\begin{vmatrix}\boldsymbol{B}_{N+1}'\\ \boldsymbol{B}_{N+1}''\end{vmatrix}=\begin{vmatrix}\boldsymbol{J}_N^{(1)} & \boldsymbol{J}_N^{(2)}\\ \boldsymbol{J}_N^{(3)} & \boldsymbol{J}_N^{(4)}\end{vmatrix}\begin{vmatrix}\boldsymbol{W}_{1,0}^{(d)}\\ \boldsymbol{W}_{1,0}^{(s)}\end{vmatrix} \quad (6)$$

Because N+1-th stratum is infinite medium in z-direction, the following condition holds.

$$\boldsymbol{B}_{N+1}{}''=0 \tag{7}$$

Then

$$\boldsymbol{W}_{1,0}{}^{(d)}=\boldsymbol{T}\boldsymbol{W}_{1,0}{}^{(s)} \tag{8}$$

where $\boldsymbol{T}=-\boldsymbol{J}_N{}^{(s)-1}\boldsymbol{J}_N{}^{(s)}$

Eq.(8) implies that displacements of surface can represent stresses of surface. The boundary conditions at surface expressed in term of stress components are:

$${}_1\sigma_{z|\bar{z}_1=0}=-\frac{P}{2\pi}e^{i\omega t}j_1{}^2\int_0^\infty \xi J_0(\xi\bar{r})d\xi \tag{9}$$

$${}_1\tau_{zr|\bar{z}_1=0}=0 \tag{10}$$

Then the response displacement of surface in case of the point load applying on the surface of soil is written as follows.

$$u_z{}^1=-\frac{Pe^{i\omega t}}{2\pi\mu_1 j}\int_0^\infty T_{21}\xi J_0(\xi\bar{r})d\xi \tag{11}$$

Finally, the Green's function of a vertical load is given as

$$G(x,y;\xi,\eta)=u_z{}^1(x-\xi,y-\eta)_{|P=1} \tag{12}$$

SOLUTION METHOD OF SOIL-STRUCTURE INTERACTION

When steady state stress $\sigma(\xi,\eta)\,e^{i\omega t}$ applies on the surface of base contact region S, the response displacement $w(x,y)e^{i\omega t}$ of the surface is represented by using the Green's function $G(x,y;\xi,\eta)$ as in Eq.(13).

$$w(x,y)e^{i\omega t}=\int_s G(x,y;\xi,\eta)\sigma(\xi,\eta)e^{i\omega t}ds \tag{13}$$

If the region S is discretized into subregion ds, Eq.(13) is transformed to

$$\{w_J\}e^{i\omega t}=[G_{IJ}]\{P_I\}e^{i\omega t} \tag{14}$$

Suppose matrix $[K_{IJ}]$ is an inverse matrix of $[G_{IJ}]$, the matrix $[K_{IJ}]$ gives dynamic stiffness matrix of soil which combines the force vector $\{P_I\}$ and the displacement vector $\{w_J\}$.

$$\{P_I\}e^{i\omega t}=[K_{IJ}]\{w_J\}e^{i\omega t} \tag{15}$$

On the other hand, the dynamic characteristics of the base mat is expressed as follows.

$$[M]\{\ddot{u}\}+[K]\{u\}=\{F\} \tag{16}$$

where $[M]$ is mass matrix, $[K]$ is stiffness matrix,
$\{u\}$ is displacement vector, $\{F\}$ is external force vector.

Consequently, the interaction analysis can be conducted by combining the matrix of base mat and soil.

$$[M]\{\ddot{u}\}+([K]+[K_{IJ}])\{u\}=\{F\} \tag{17}$$

NUMERICAL CALCULATIONS AND DISCUSSIONS

The dynamic behaviors of a reinforced concrete base mat subject to the harmonically vertical ground motion are analyzed.
That is, external force vector:

$\{F\}=[M]\{I\}\ddot{\alpha}e^{i\omega t}$

$\{I\}=$ unit vector

$\ddot{\alpha}=$ earthquake acceleration, in this case $\ddot{\alpha}=1$gal

The base mat is a square with 80m side length and 7m thickness. One fourth of soil-base mat system is considered according to its symmetry. Two kinds of soil conditions are considered as shown in Fig.3. The case 1 soil consists of three strata. The case 2 soil is a semi-infinite homogeneous isotropic medium with equivalent s-wave velocity to case 1 soil. The physical constants are summarized in Table 1. In regard to damping, the base mat has the complex rigidity with 5% damping and soil of both cases 3% hysteresis type damping.

Fig.4 to Fig.9 show the frequency transfer functions of each part of base mats. In those figures, real line represent of the result of case 1 soil condition, and dot line represent of the result of case 2 soil condition. The discrepancies of two curves are caused by the existence of layered strata. While the base mat on case 2 soil has smooth transfer functions, these functions for case 1 soil became curves which have a peak at nearly 4.5Hz. This peak reflects the dynamic characteristics of layered strata. The phase angle curves for case 1 soil is very complex.

To investigate the elastic deformations of a base mat on case 1 soil, the transfer functions of each point are summarized in Fig.10 and Fig.11. The functions are remarkably different. Therefore, the base mat does not vibrate as a rigid body, but the elastic deformations considerably occur.

Fig.12 to Fig.15 show patterns of response displacement of the base mat at the beginning ($t=2n\pi/\omega$) of steady state excitation. They show that displacements of base mat differ depending frequency and the existence of soil layers.

Fig.16 to Fig.19 show patterns of reaction stresses of the base mat at the beginning of steady state excitation. Similar to response displacement, reaction stresses of the base mat differ depending frequency and the existence of soil layers.

CONCLUDING REMARKS

The solution method is presented to estimate the dynamic behaviors of base mat resting on layered strata. The followings can be drawn from the present numerical results.

(1) The elastic deformations and contact pressures for a base mat resting on layered strata are considerably different from those on non-layered stratum. The numerical calculation taking into account of layered strata must be performed to precisely estimate the dynamic behaviors of base mat.

(2) The base mat induces the large elastic deformations. Therefore, the conventional methods are not enough where the rigid condition of base mat or the contact pressure are assumed a priori.

REFERENCE

1. T.Kobori, R.Minai, T.Suzuki; Dynamic Characteristics of a Layered Sub-Soil Ground (in Japanese), Report of Kyoto Univ., Vol.19, 1976
2. J.E.Luco; Vibrations of a Rigid Disc on a Layered Viscoelastic Medium, Nuclear Engineering and Design, Vol.36, 1976
3. A.K.Chopra, P.Chakrabarti, G.Dasgupta; Dynamic Stiffness Matrices for Viscoelastic Half-Plane Foundation, J.Eng.Mech.Division, ASCE, EM3,1976
4. G.Gazetas; Strip Foundations on a Cross-Anisotropic Soil Layer Subjected to Dynamic Loading, Géotechnique, Vol.31, 1981
5. S.Krenk, H.Schmidt; Vibration of an Elastic Circular Plate on an Elastic Half Space--A Direct Approach, J.Applied Mechanics, ASME, Vol.48, 1981
6. W.L.Whittaker, P.Christiano; Dynamic Response of Plate on Elastic Half-Space, J.Eng.Mech.Division, ASCE, EM1, 1982

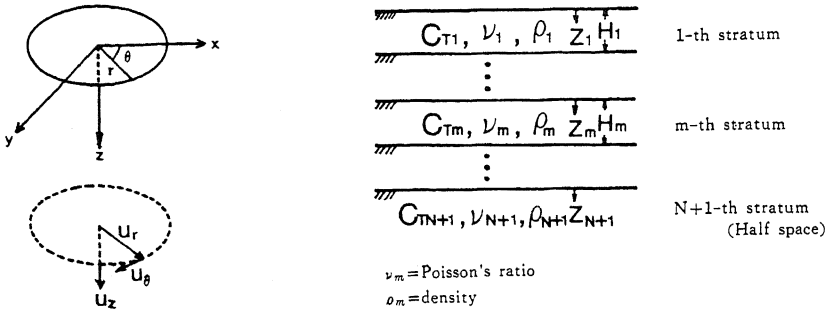

Fig. 1 COORDINATE SYSTEM

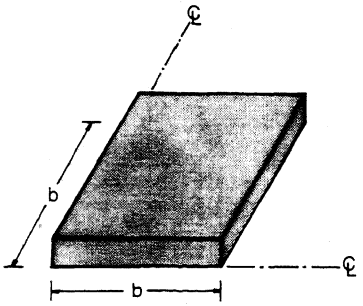

HALF LENGTH OF BASE MAT	40m
THICKNESS	7m
YOUNG'S MODULUS	210ton/m
DENSITY	2.4ton/m³

Fig. 2. BASE MAT 1/4 MODEL

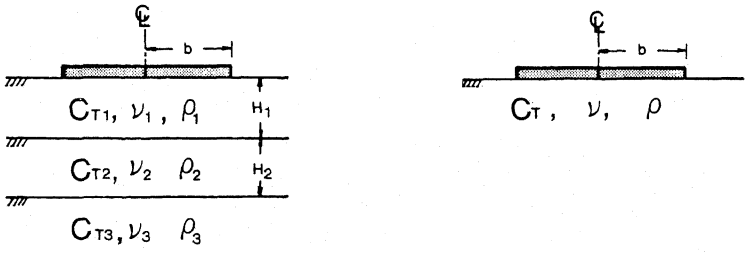

Fig. 3 SOIL MODEL

TABLE 1 PHISICAL CONSTANTS OF SOIL

	STRATUM	C_{Tm}	ν_m	ρ_m	H_m
Case1	1-th	500 m/sec	0.4	2.0 ton/m³	40 m
	2-th	1000 m/sec	0.4	2.0 ton/m³	40 m
	3-th	2000 m/sec	0.4	2.0 ton/m³	
Case2	HALE SPACE	800m/sec	0.4	2.0 ton/m³	

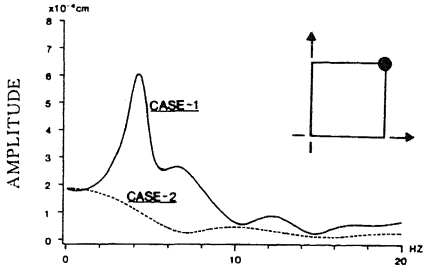

Fig. 4 TRANSFER FUNCTION

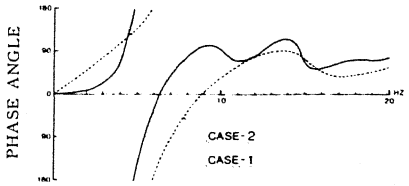

Fig. 5 TRANSFER FUNCTION

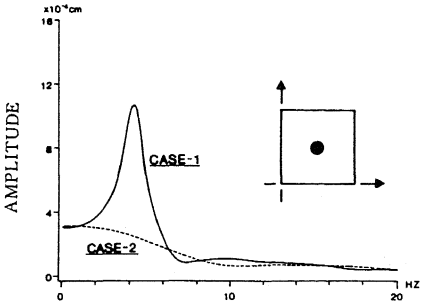

Fig. 6 TRANSFER FUNCTION

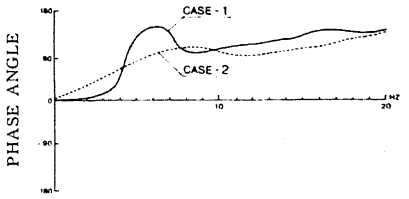

Fig. 7 TRANSFER FUNCTION

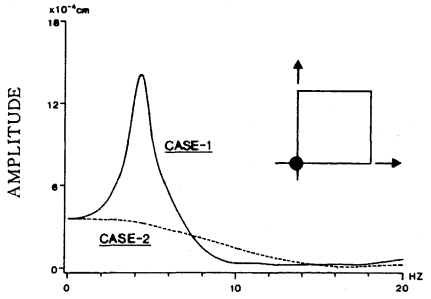

Fig. 8 TRANSFER FUNCTION

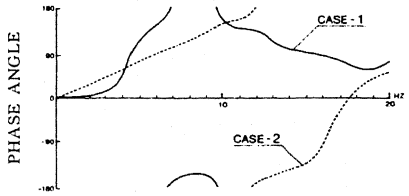

Fig. 9 TRANSFER FUNCTION

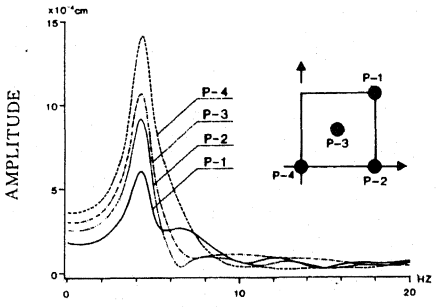

Fig. 10 TRANSFER FUNCTION (case 1)

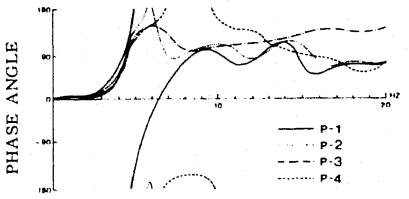

Fig. 11 TRANSFER FUNCTION (case 1)

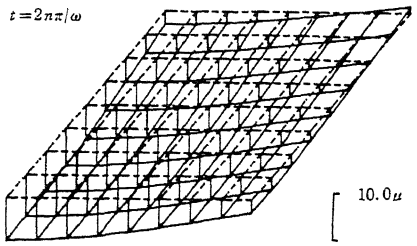

Fig. 12 RESPONSE DISPLACEMENT CASE 1 5Hz

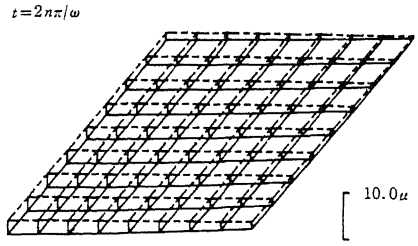

Fig. 13 RESPONSE DISPLACEMENT CASE 2 5Hz

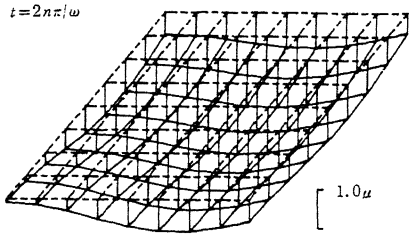

Fig. 14 RESPONSE DISPLACEMENT CASE 1 10Hz

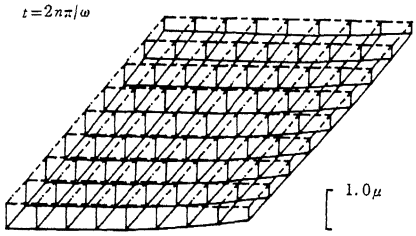

Fig. 15 RESPONSE DISPLACEMENT CASE 2 10Hz

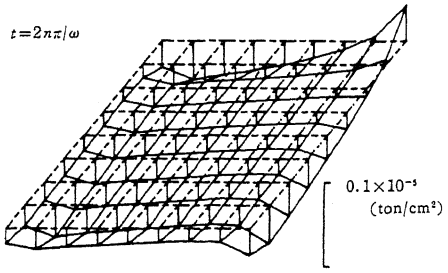

Fig. 16 RESPONSE REACTION FORCE CASE 1 5Hz

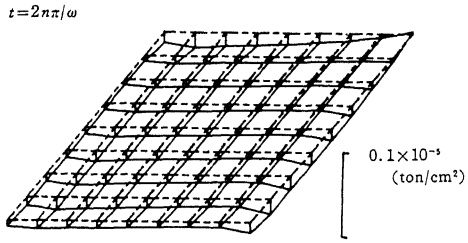

Fig. 17 RESPONSE REACTION FORCE CASE 2 5Hz

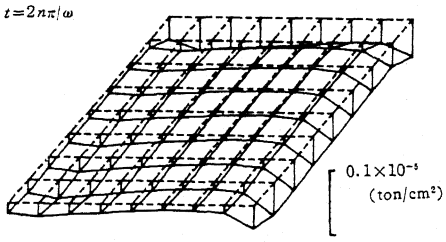

Fig. 18 RESPONSE REACTION FORCE CASE 1 10Hz

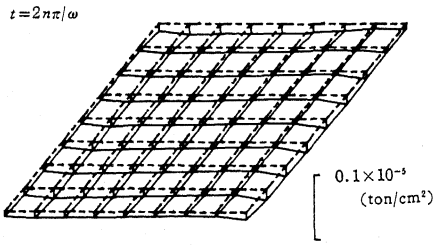

Fig. 19 RESPONSE REACTION FORCE CASE 2 10Hz